We are IntechOpen,
the world's leading publisher of
Open Access books
Built by scientists, for scientists

6,900
Open access books available

186,000
International authors and editors

200M
Downloads

Our authors are among the

154
Countries delivered to

TOP 1%
most cited scientists

12.2%
Contributors from top 500 universities

CLARIVATE ANALYTICS
BOOK CITATION INDEX
INDEXED

WEB OF SCIENCE™

Selection of our books indexed in the Book Citation Index
in Web of Science™ Core Collection (BKCI)

Interested in publishing with us?
Contact book.department@intechopen.com

Quantal Cumulant Mechanics as Extended Ehrenfest Theorem

Yasuteru Shigeta

Additional information is available at the end of the chapter

1. Introduction

Since Schrödinger proposed wave mechanics for quantum phenomena in 1926 [1-4], referred as Schrödinger equation named after his name, this equation has been applied to atom-molecules, condensed matter, particle, and elementary particle physics and succeeded to reproduce various experiments. Although the Schrödinger equation is in principle the differential equation and difficult to solve, by introducing trial wave functions it is reduced to matrix equations on the basis of the variational principle. The accuracy of the approximate Schrödinger equation depends strongly on the quality of the trial wave function. He also derived the time-dependent Schrödinger equation by imposing the time-energy correspondence. This extension opened to describe time-dependent phenomena within quantum mechanics. However there exist a few exactly solvable systems so that the methodology to solve Schrödinger equation approximately is extensively explored, yet.

In contrast to the time-dependent wave mechanics, Heisenberg developed the equations of motion (EOM) derived for time-dependent operator rather than wave function [5]. This equation is now referred as the Heisenberg' EOM. This equation is exactly equivalent to the time-dependent Schrödinger equation so that the trials to solve the Heisenberg' EOM rather than Schrödinger one were also done for long time. For example, the Dyson equation, which is the basic equation in the Green's function theory, is also derived from the Heisenberg' EOM. Various approximate methods were deviced to solve the Dyson equation for nuclear and electronic structures.

In this chapter, we propose a new approximate methodology to solve dynamical properties of given systems on the basis of quantum mechanics starting from the Heisenberg' EOM. First, theoretical background of the method is given for one-dimensional systems and an extension to multi-dimensional cases is derived. Then, we show three applications in molecu-

lar physics, i.e. the molecular vibration, the proton transfer reaction, and the quantum structural transition, respectively. Finally, we give conclusion at the last part.

2. Theoretical background

2.1. Heisenberg' equation of motion and Ehrenfest theorem

When the Hamiltonian does not explicitly depend on time, by defining time-dependent of an arbitrary operator A in the Heisenberg representation as

$$\hat{A}(t) = e^{-\frac{i}{\hbar}\hat{H}t}\hat{A}(0)e^{\frac{i}{\hbar}\hat{H}t}.$$ (1)

The Heisenberg' equation of motion (EOM) is given as

$$\frac{\partial \hat{A}(t)}{\partial t} = \frac{1}{i\hbar}\left[\hat{A}(t),\hat{H}\right],$$ (2)

where $\hat{H}$ is the Hamiltonian operator and $h = 2\pi\hbar$ is the Planck's constant. As an expectation value of A with respect to ψ is expressed as $\langle A \rangle \equiv \langle \psi \mid \hat{A} \mid \psi \rangle$, the Heisenberg' EOM is rewritten as

$$\frac{\partial \langle \hat{A}(t)\rangle}{\partial t} = \frac{1}{i\hbar}\left\langle\left[\hat{A}(t),\hat{H}\right]\right\rangle \equiv \frac{1}{i\hbar}\left\langle e^{-\frac{i}{\hbar}\hat{H}t}\left[\hat{A},\hat{H}\right]e^{\frac{i}{\hbar}\hat{H}t}\right\rangle.$$ (3)

For one-dimensional case, the Hamiltonian operator is expressed as a sum of the kinetic and the potential operator as

$$\hat{H} = \frac{\hat{p}^2}{2m} + V(\hat{q}).$$ (4)

The Heisenberg' EOMs for both a coordinate and a momentum are derived as

$$\begin{cases} \dfrac{\partial \langle \hat{q}(t)\rangle}{\partial t} = \dfrac{\langle \hat{p}(t)\rangle}{m} \\ \dfrac{\partial \langle \hat{p}(t)\rangle}{\partial t} = -\left\langle V^{(1)}(\hat{q}(t))\right\rangle \end{cases} \rightarrow \begin{cases} \dot{q}(t) = \dfrac{p(t)}{m} \\ \dot{p}(t) = -\left\langle V^{(1)}(\hat{q}(t))\right\rangle \end{cases}.$$ (5)

These equations resemble corresponding Newton' EOMs as

$$\dot{q}(t) = \frac{p(t)}{m}$$
$$\dot{p}(t) = -V^{(1)}(q(t)). \tag{6}$$

This relationship is so-called Ehrenfest's theorem [6]. A definite difference between Heisenberg' and Nowton' EOMs is that the expectation value of the potential operator appears in the former. If one approximates the expectation value as

$$\left\langle V\left(\hat{q}(t)\right)\right\rangle \approx V\left(\left\langle \hat{q}(t)\right\rangle\right), \tag{7}$$

the same structure of the EOM is immediately derived. However, there is no guarantee that this approximation always holds for general cases. Including this approximation is also referred as the Ehrenfest's theorem.

In general, Taylor expansion of the potential energy term,

$$\left\langle V\left(\hat{q}(t)\right)\right\rangle = V(0) + V^{(1)}(0)\left\langle \hat{q}(t)\right\rangle + \frac{1}{2!}V^{(2)}(0)\left\langle \hat{q}^2(t)\right\rangle + \frac{1}{3!}V^{(3)}(0)\left\langle \hat{q}^3(t)\right\rangle + \cdots, \tag{8}$$

gives a infinite series of higher-order derivatives, $V^{(m)}(0)$, times expectation values of higher-powers of coordinate moment operators, $\left\langle \hat{q}^m(t)\right\rangle$ ($m=1, 2, \cdots$). Introducing a fluctuation operator of A as $\delta A \equiv A - \langle A\rangle$ and the expectation values of the higher-order central moment $\left\langle \delta\hat{q}^m(t)\right\rangle \equiv \left\langle (\hat{q}(t) - \langle\hat{q}(t)\rangle)^m\right\rangle$ ($m=2, 3, \cdots$), the Taylor series is rewritten as

$$\left\langle V\left(\hat{q}(t)\right)\right\rangle = V\left(\left\langle\hat{q}(t)\right\rangle\right) + \frac{1}{2!}V^{(2)}\left(\left\langle\hat{q}(t)\right\rangle\right)\left\langle\delta\hat{q}^2(t)\right\rangle + \frac{1}{3!}V^{(3)}\left(\left\langle\hat{q}(t)\right\rangle\right)\left\langle\delta\hat{q}^3(t)\right\rangle + \cdots, \tag{9}$$

The first term appears in Eq. (2-7) and the other terms are neglected by the approximation made before. This relation indicates that the difference between classical mechanics and quantum mechanics is existence of higher-order moment.

2.2. Quantized Hamilton dynamics and quantal cumulant dynamics

Ehrenfest' theorem fulfills for the arbitrary wave function. In previous studies, effects of the higher-order moments on dynamics were explored. The most of studies treat second-order

term with the potential being a series of q. For example, Prezhdo and co-workers derived EOMs for three additional moments of $\langle \hat{q}^2(t) \rangle$, $\langle \hat{p}^2(t) \rangle$, and $\langle (\hat{q}(t)\hat{p}(t))_s \rangle$ and solved the EOMs by truncating the potential term up to fourth-order power series. The subscript s represent a symmetric sum of the operator product defined as $\langle (\hat{q}(t)\hat{p}(t))_s \rangle = \frac{1}{2} \langle (\hat{q}(t)\hat{p}(t) + \hat{p}(t)\hat{q}(t)) \rangle$. Judging from previous works, this formalism is essentially the same as Gaussian wave packet method. Prezhdo also proposed a correction to the higher-order moments [8]. Nevertheless their formalism could not be applied general potential without any approximation such as the truncation.

Recently Shigeta and co-workers derived a general expression for the expectation value of an arbitrary operator by means of cumulants rather than moments [9-19]. For one-dimensional case, the expectation value of a differential arbitrary operator, $A_s(\hat{q}, \hat{p})$, that consists of the symmetric sum of power series of q and p is derived as

$$\left\langle A_s\left(\hat{q}(t),\hat{p}(t)\right)\right\rangle = \exp\left(\sum_m \sum_{0 \leq l \leq m} \frac{\lambda_{l,m-l}(t)}{l!(m-l)!} \frac{\partial^m}{\partial q^l \partial p^{m-l}}\right) A(q,p), \tag{10}$$

where we introduced the general expression for the cumulant $\lambda_{m,n}(t) \equiv \langle (\delta \hat{q}^m(t) \delta \hat{p}^n(t))_s \rangle$, in which the subscripts mean m-th order and n-th order with respect to the coordinate and momentum, respectively [20-22]. Using the expression, the expectation value of the potential is

$$\left\langle V\left(\hat{q}(t)\right)\right\rangle = \exp\left(\sum_{m=2} \frac{\lambda_{m,0}(t)}{m!} \frac{\partial^m}{\partial q^m}\right) V(q). \tag{11}$$

Thus, when the anharmonicity of the potential is remarkable, it is expected that the higher-order cumulants play important role in their dynamics. Indeed, for the harmonic oscillator case, only the second-order cumulant appears as

$$\left\langle V\left(\hat{q}(t)\right)\right\rangle = \frac{m\omega^2}{2}\left(q(t)^2 + \lambda_{2,0}(t)\right), \tag{12}$$

and the other higher-order terms do not.

Up to the second-order, Heisenberg' EOMs for cumulants are given by

$$
\begin{cases}
\dot{q}(t) = \dfrac{p(t)}{m} \\[2mm]
\dot{p}(t) = -\tilde{V}^{(1,0)}\big(q(t), \lambda_{2,0}(t)\big) \\[2mm]
\dot{\lambda}_{2,0}(t) = \dfrac{2\lambda_{1,1}(t)}{m} \\[2mm]
\dot{\lambda}_{1,1}(t) = \dfrac{\lambda_{0,2}(t)}{m} - \lambda_{2,0}(t)\tilde{V}^{(2,0)}\big(q(t), \lambda_{2,0}(t)\big) \\[2mm]
\dot{\lambda}_{0,2}(t) = -2\lambda_{1,1}(t)\tilde{V}^{(2,0)}\big(q(t), \lambda_{2,0}(t)\big)
\end{cases}
\tag{13}
$$

where $\widetilde{V}$ is second-order "quantal" potential defined as

$$
\tilde{V}\big(q(t), \lambda_{2,0}(t)\big) \equiv \big\langle V\big(\hat{q}(t)\big)\big\rangle_2 = \exp\!\left(\frac{\lambda_{2,0}}{2}\frac{\partial^2}{\partial q^2}\right)V(q)\bigg|_{q=\langle\hat{q}(t)\rangle}.
\tag{14}
$$

$\widetilde{V}^{(n,0)}$ is the n-th derivative of $\widetilde{V}$ with respect to q. It is easily seen that the quantal potential is a finite series with respect to the cumulant by expanding as a Taylor series as

$$
\big\langle V\big(\hat{q}(t)\big)\big\rangle_2 = V\big(\langle\hat{q}(t)\rangle\big) + \frac{\lambda_{2,0}}{2}V^{(2)}\big(\langle\hat{q}(t)\rangle\big) + \frac{\lambda_{2,0}^2}{8}V^{(4)}\big(\langle\hat{q}(t)\rangle\big) + \cdots,
\tag{15}
$$

It is noteworthy that the first and second terms of above equation corresponds to the first and second terms of Eq. (2-9), on the other hand, the other term are different each other.

Now we here give an expression to the quantal potential that has complicated form like as in Eq. (2-14). By using the famous formula for the Gaussian integral

$$
\int_{-\infty}^{\infty}\exp\!\left[-\big(ar^2 + br\big)\right]dr = \int_{-\infty}^{\infty}\exp\!\left[-a\left(r + \frac{b}{2a}\right)^2 + \frac{b^2}{4a}\right]dr = \sqrt{\frac{\pi}{a}}\exp\!\left(\frac{b^2}{4a}\right),
\tag{16}
$$

the exponential operator appearing in Eq. (2-14) is rewritten as,

$$
\exp\!\left(\frac{\lambda_{2,0}}{2}\frac{\partial^2}{\partial q^2}\right) = \frac{1}{\sqrt{2\pi\lambda_{2,0}}}\int_{-\infty}^{\infty}\exp\!\left[-\left(\frac{r^2}{2\lambda_{2,0}} + r\frac{\partial}{\partial q}\right)\right]dr.
\tag{17}
$$

The first derivative operator term in right hand side of the above equation can act to the potential with the relationship of $\exp\left[r\frac{\partial}{\partial q}\right]f(q)=f(q+r)$ as

$$\exp\left(\frac{\lambda_{2,0}}{2}\frac{\partial^2}{\partial q^2}\right)V(q)=\int_{-\infty}^{\infty}\frac{dr}{\sqrt{2\pi\lambda_{2,0}}}\exp\left[-\frac{r^2}{2\lambda_{2,0}}\right]V(q+r)$$

$$=\int_{-\infty}^{\infty}\frac{dr}{\sqrt{2\pi\lambda_{2,0}}}\exp\left[-\frac{(q-r)^2}{2\lambda_{2,0}}\right]V(r). \tag{18}$$

Therefore it is possible to estimate potential energy term without the truncation of the potential. However the analytic integration is not always has the closed form and the numerical integration does not converge depending on the kind of the potential. For the quantal potential including third and higher-order culumant, it is convenient to use the Fourier integral instead of Gaussian integral. Nevertheless this scheme also has problems concerning about the integrability and its convergence.

2.3. Energy conservation law and least uncertainty state

For the EOMs of Eq. (2-13), there exists first integral that always hold for. Now defining a function,

$$\gamma(t)=\lambda_{2,0}(t)\lambda_{0,2}(t)-\lambda_{1,1}^2(t), \tag{19}$$

and differentiating it result in

$$\begin{aligned}\dot{\gamma}(t)&=\dot{\lambda}_{2,0}(t)\lambda_{0,2}(t)+\lambda_{2,0}(t)\dot{\lambda}_{0,2}(t)-2\lambda_{1,1}(t)\dot{\lambda}_{1,1}(t)\\&=\frac{2\lambda_{1,1}(t)}{m}\lambda_{0,2}(t)-2\lambda_{2,0}\lambda_{1,1}(t)V^{(2,0)}\big(q(t),\lambda_{2,0}(t)\big)\\&\quad-2\lambda_{1,1}(t)\left\{\frac{\lambda_{0,2}(t)}{m}-\lambda_{0,2}(t)V^{(2,0)}\big(q(t),\lambda_{2,0}(t)\big)\right\}\\&=0.\end{aligned} \tag{20}$$

Thus, this function is a time-independent constant. It is well-known that the least uncertainty state fulfills $\gamma=\frac{\hbar^2}{4}$. By setting the adequate parameter, one can incorporate the Heisenberg' uncertainty principle and thus least uncertainty relation into EOMs. Using this value, one can delete one cumulant from EOMs, for example

$$\lambda_{0,2}(t) = \frac{\lambda_{1,1}^2(t)}{\lambda_{2,0}(t)} + \frac{\hbar^2}{4\lambda_{2,0}(t)}. \tag{21}$$

Now by considering the dimension we define new coordinate and momentum as

$$p_\lambda(t) = \frac{\lambda_{1,1}(t)}{\sqrt{\lambda_{2,0}(t)}}$$
$$q_\lambda(t) = \sqrt{\lambda_{2,0}(t)}. \tag{22}$$

The second-order momentum cumulant $\lambda_{0,2}(t)$ is rewritten using them as

$$\lambda_{0,2}(t) = p_\lambda^2(t) + \frac{\hbar^2}{4q_\lambda^2(t)}. \tag{23}$$

Total energy are expressed using the cumulant variables as

$$E_2(t) = \langle H \rangle_2 = \frac{p^2(t) + \lambda_{0,2}(t)}{2m} + \int \frac{dr}{\sqrt{2\pi\lambda_{2,0}(t)}} \exp\left(-\frac{(r-q(t))^2}{2\lambda_{2,0}(t)}\right) V(r). \tag{24}$$

Above expression indicates that the energy does not depend on $\lambda_{1,1}(t)$. Differentiating the energy with respect to time gives the energy conservation law. The proof of the energy conservation law is give below.

$$\dot{E}_2(t) = \frac{2\dot{p}(t)p(t) + \dot{\lambda}_{0,2}(t)}{2m} - \dot{q}(t)\int \frac{dr}{\sqrt{2\pi\lambda_{2,0}(t)}} \frac{(r-q(t))}{\lambda_{2,0}(t)} \exp\left(-\frac{(r-q(t))^2}{2\lambda_{2,0}(t)}\right) V(r).$$
$$+ \int \frac{dr}{\sqrt{2\pi\lambda_{2,0}^3(t)}} \dot{\lambda}_{2,0}(t)\left(1 + \frac{(r-q(t))^2}{2\lambda_{2,0}(t)}\right) \exp\left(-\frac{(r-q(t))^2}{2\lambda_{2,0}(t)}\right) V(r) \tag{25}$$
$$= 0$$

By means of the new coordinate and momentum, the total energy is rewritten as

$$E_2 = \frac{p^2(t) + p_\lambda^2(t)}{2m} + \frac{\hbar^2}{8mq_\lambda^2(t)} + \frac{1}{q_\lambda(t)} \int \frac{dr}{\sqrt{2\pi}} \exp\left(-\frac{(r-q(t))^2}{2q_\lambda^2(t)}\right) V(r). \tag{26}$$

This equation tells us that the effective potential derived from the kinetic energy term affect the dynamics of $q(t)$ via dynamics of $q_\lambda(t)$. A variational principle of E_2,

$$\frac{\partial E_2}{\partial p} = \frac{\partial E_2}{\partial p_\lambda} = \frac{\partial E_2}{\partial q} = \frac{\partial E_2}{\partial q_\lambda} = 0, \tag{27}$$

gives stationary state that fulfills the least uncertainty condition as

$$\frac{\partial E_2}{\partial p} = \frac{p}{m} = 0.$$
$$\frac{\partial E_2}{\partial p_\lambda} = \frac{p_\lambda}{m} = 0$$
$$\frac{\partial E_2}{\partial q} = V_2^{(1,0)}(q, q_\lambda) = 0 \tag{28}$$
$$\frac{\partial E_2}{\partial q_\lambda} = -\frac{\hbar^2}{4mq_\lambda^3} + q_\lambda V_2^{(2,0)}(q, q_\lambda) = 0$$

For both momenta, the solutions of the above variational principle are zero. On the other hand, the solutions for the coordinates strongly depend on the shape of the give potential. As an exactly soluble case, we here consider the harmonic oscillator. The variational condition gives a set of solutions as $(p, p_\lambda, q, q_\lambda) = (0, 0, 0, \sqrt{\hbar/2m\omega})$. The corresponding energy $E_2 = \frac{\hbar\omega}{2}$ is the same as the exact ground state energy. The cumulant variables estimated from the solutions result in $(\lambda_{2,0}, \lambda_{1,1}, \lambda_{0,2}) = \left(\frac{\hbar}{2m\omega}, 0, \frac{m\hbar\omega}{2}\right)$ being the exact expectation values for the ground state. Thus the present scheme with the least uncertainty relation is reasonable at least for the ground state.

2.4. Distribution function and joint distribution

In order to visualize the trajectory in this theory, we here introduce distribution function as a function of coordinate and second-order cumulant variables. Now the density finding a

particle at r is the expectation value of the density operator, $\delta(\hat{q}-r)$, with a useful expression as

$$\rho(r)=\left\langle\delta(\hat{q}-r)\right\rangle=\lim_{\beta\to\infty}\sqrt{\frac{\beta}{\pi}}\left\langle\exp\left(-\beta(\hat{q}-r)^2\right)\right\rangle. \tag{29}$$

Thus the second-order expression for the density is evaluated as

$$\rho_2(r)=\frac{1}{\sqrt{2\pi\lambda_{2,0}}}\exp\left(-\frac{1}{2\lambda_{2,0}}(r-q)^2\right). \tag{30}$$

This density shows that the distribution is a Gaussian centered at q with a width depending on the cumulant $\lambda_{2,0}$. Thus the physical meaning of the second-order cumulant $\lambda_{2,0}$ results in the width of the distribution. As the integration of this density for the whole space becomes unity, the density is normalized. Therefore the density has the physical meaning of probability. Comparison with Eq. (2-18), the potential energy is rewritten by means of the density as

$$\left\langle V(\hat{q})\right\rangle_2=\int\frac{dr}{\sqrt{2\pi\lambda_{2,0}}}\exp\left(-\frac{(r-q)^2}{2\lambda_{2,0}}\right)V(r)\equiv\int dr\rho_2(r)V(r). \tag{31}$$

This expression indicates that the expectation value of the potential is related to the mean average of the potential with weight $\rho_2(r)$. The same relationship holds for the momentum distribution.

In principle, one cannot determine the position and momentum at the same time within the quantum mechanics. In other words, resolution of phase space is no more than the Planck' constant, h. In contrast to the quantum mechanics, we can define the joint distribution function on the basis of the present theory as

$$\rho_{\text{joint}}(r,s)=\left\langle\left(\delta(\hat{q}-r)\delta(\hat{p}-s)\right)_s\right\rangle. \tag{32}$$

The second-order expression is given by

$$\rho_{\text{joint}}(r,s)=\frac{1}{2\pi\sqrt{\gamma}}\exp\left[-\frac{\lambda_{0,2}(r-q)^2-2\lambda_{1,1}(r-q)(s-p)+\lambda_{2,0}(s-p)^2}{2\gamma}\right]. \tag{33}$$

In contrast to the energy, the joint distribution depends on all the cumulant variables. In the phase space, this joint distribution has the elliptic shape rotated toward *r-s* axes. This joint distribution corresponds not to a simple coherent state, but to a squeezed-coherent state.

Using the joint distribution, the expectation value of the arbitrary operator is evaluated via

$$\left\langle A_s\left(\hat{q},\hat{p}\right)\right\rangle = \iint A(r,s)\rho_{\text{joint}}(r,s)drds. \tag{34}$$

In this sense, this theory is one of variants of the quantum distribution function theory. This joint distribution fulfills the following relations as

$$\int \rho_{\text{joint}}(r,s)ds = \rho(r)$$
$$\int \rho_{\text{joint}}(r,s)dr = \rho_{\text{momentum}}(s) \tag{35}$$
$$\iint \rho_{\text{joint}}(r,s)drds = 1.$$

Moreover the coordinate, momentum, and cumulants are derived by means of the joint distribution as

$$q = \iint r\rho_{\text{joint}}(r,s)drds$$
$$p = \iint s\rho_{\text{joint}}(r,s)drds$$
$$\lambda_{2,0} = \iint (r-q)^2 \rho_{\text{joint}}(r,s)drds \tag{36}$$
$$\lambda_{1,1} = \iint (r-q)(s-p)\rho_{\text{joint}}(r,s)drds$$
$$\lambda_{0,2} = \iint (s-p)^2 \rho_{\text{joint}}(r,s)drds.$$

2.5. Extension to multi-dimensional systems

The Hamiltonian of an *n*-dimensional *N* particle system including a two-body interaction is written by

$$\hat{H} = \sum_{I=1}^{N}\frac{\hat{\mathbf{P}}_I^2}{2m_I} + \sum_{I>J}^{N}V\left(\left\|\hat{\mathbf{Q}}_I - \hat{\mathbf{Q}}_J\right\|\right), \tag{37}$$

where $\hat{\mathbf{Q}}_I = \left(\hat{q}_{I1}, \hat{q}_{I2}, \cdots, \hat{q}_{In}\right)$ and $\hat{\mathbf{P}}_I = \left(\hat{p}_{I1}, \hat{p}_{I2}, \cdots, \hat{p}_{In}\right)$, and m_I represent a vector of *I*-th position operator, that of momentum operator, and mass, respectively. We here assume that the potential $V(r)$ is a function of the inter-nuclear distance *r*. Using the definitions of the second-order single-particle cumulants given by

$$\xi_{I,kl} = \left\langle \left(\delta \hat{q}_{Ik} \delta \hat{q}_{Il} \right)_s \right\rangle$$
$$\eta_{I,kl} = \left\langle \left(\delta \hat{p}_{Ik} \delta \hat{p}_{Il} \right)_s \right\rangle, \qquad (38)$$
$$\zeta_{I,kl} = \left\langle \left(\delta \hat{q}_{Ik} \delta \hat{p}_{Il} \right)_s \right\rangle$$

the total energy is derived as an extension of Eq. (2-26) by

$$E_2 = \sum_{I=1}^{N} \frac{\mathbf{P}_I^2 + \boldsymbol{\eta}_I \cdot \mathbf{1}_n}{2m_I} + \sum_{I>J}^{N} \tilde{V}_2 \left(\mathbf{Q}_I - \mathbf{Q}_J, \boldsymbol{\xi}_I + \boldsymbol{\xi}_J \right), \qquad (39)$$

where P_I and Q_I are n-dimensional momentum and coordinae and $\mathbf{1}_n = (1 \quad 1 \quad \cdots \quad 1)$ is n-dimensional identity vector. $V(Q, \xi)$ is the second-order quantal potential given as

$$\tilde{V}_2 \left(\mathbf{Q}, \boldsymbol{\xi} \right) = \int \frac{d\mathbf{r}}{\sqrt{(2\pi)^n \det |\boldsymbol{\xi}|}} \exp\left(-\frac{1}{2} (\mathbf{Q} - \mathbf{r})^T \boldsymbol{\xi}^{-1} (\mathbf{Q} - \mathbf{r}) \right) V(|\mathbf{r}|), \qquad (40)$$

where ξ is an n by n matrix composed of the position cumulant variables. From Heisenberg uncertainty relation and the least uncertainty, the total energy of Eq. (2-39) is rewritten as

$$E_2^{LQ} = \sum_{I=1}^{N} \frac{\mathbf{P}_I^2}{2m_I} + \sum_{i} \frac{\hbar^2}{8m_I} \mathrm{Tr}\left(\boldsymbol{\xi}_I^{-1} \right) + \sum_{I>J}^{N} \tilde{V}_2 \left(\mathbf{Q}_I - \mathbf{Q}_J, \boldsymbol{\xi}_I + \boldsymbol{\xi}_J \right). \qquad (41)$$

From Heisenberg EOM, EOMs up to the second-order cumulants are given by

$$\dot{q}_{Ik} = \frac{p_{Ik}}{m_I}$$
$$\dot{p}_{Ik} = -\tilde{W}_2^{(1_{Ik})} \left(\{\mathbf{q}_I - \mathbf{q}_J\}, \{\boldsymbol{\xi}_I + \boldsymbol{\xi}_J\} \right)$$
$$\dot{\xi}_{I,kl} = \frac{\zeta_{I,kl} + \zeta_{I,lk}}{m_I} \qquad (42)$$
$$\dot{\eta}_{I,kl} = -\sum_m \left[\zeta_{I,ml} \tilde{W}_2^{(2_{Im,Ik})} \left(\{\mathbf{q}_I - \mathbf{q}_J\}, \{\boldsymbol{\xi}_I + \boldsymbol{\xi}_J\} \right) + \zeta_{I,mk} \tilde{W}_2^{(2_{Im,Il})} \left(\{\mathbf{q}_I - \mathbf{q}_J\}, \{\boldsymbol{\xi}_I + \boldsymbol{\xi}_J\} \right) \right]$$
$$\dot{\zeta}_{I,kl} = \frac{\eta_{I,kl}}{m_I} - \sum_m \xi_{i,km} \tilde{W}_2^{(2_{Im,Il})} \left(\{\mathbf{q}_I - \mathbf{q}_J\}, \{\boldsymbol{\xi}_I + \boldsymbol{\xi}_J\} \right),$$

where $\widetilde{W}_2^{(1_{Ik})}(\{\mathbf{Q}_I-\mathbf{Q}_J\}, \{\xi_I+\xi_J\})$ and $\widetilde{W}_2^{(2_{Ik,Im})}(\{\mathbf{Q}_I-\mathbf{Q}_J\}, \{\xi_I+\xi_J\})$ are the 1st and 2nd derivatives of the sum of the quantal potentials with respect to the position q_{ik} and to q_{ik} and q_{im} defined as

$$
\begin{aligned}
\tilde{W}_2^{(1_{Ik})}\left(\left\{\mathbf{Q}_I-\mathbf{Q}_J\right\},\left\{\xi_I+\xi_J\right\}\right) &= \sum_J \frac{\partial \tilde{V}_2\left(\mathbf{Q}_I-\mathbf{Q}_J, \xi_I+\xi_J\right)}{\partial q_{Ik}} \\
\tilde{W}_2^{(2_{Ik,Im})}\left(\left\{\mathbf{Q}_I-\mathbf{Q}_J\right\},\left\{\xi_I+\xi_J\right\}\right) &= \sum_J \frac{\partial^2 \tilde{V}_2\left(\mathbf{Q}_I-\mathbf{Q}_J, \xi_I+\xi_J\right)}{\partial q_{Ik}\partial q_{Im}}.
\end{aligned}
\tag{43}
$$

In contrast to the one-dimensional problems, second-order cumulants are represented as matrices. Thus, the total degrees of freedom are 24N for 3-dimensional cases. For the latter convenience, we here propose two different approximations. The one is the diagonal approximation, where the all off-diagonal elements are neglected, and the spherical approximation, where the all diagonal cumulants are the same in addition to the diagonal approximation. In the following, we apply the present methods for several multi-dimensional problems. We hereafter refer our method as QCD2.

3. Applications

3.1. Application to molecular vibration

Here we evaluate the vibrational modes from the results obtained from molecular dynamics (MD) simulations. Since the force field based model potentials, which are often used in molecular dynamics simulations, are empirical so that they sometimes leads to poor results for molecular vibrations. For quantitative results in any MD study, the accuracy of the PES is the other important requirement as well as the treatment of the nuclear motion. Here we use an efficient representation of the PES derived from *ab initio* electronic structure methods, which is suitable for both molecular vibration and the QCD scheme in principle. In order to include anharmonic effects, multi-dimensional quartic force field (QFF) approximation [23] is applied as

$$
V_{\mathrm{QFF}}\left(\left\{\hat{Q}_i\right\}\right) = V_0 + \sum_i \frac{h_{ii}}{2}\hat{Q}_i^2 + \sum_{ijk} \frac{t_{ijk}}{6}\hat{Q}_i\hat{Q}_j\hat{Q}_k + \sum_{ijkl} \frac{u_{ijkl}}{24}\hat{Q}_i\hat{Q}_j\hat{Q}_k\hat{Q}_l,
\tag{44}
$$

where V_0, h_{ii}, t_{ijk}, and u_{ijkl} denote the potential energy and its second-, third- and fourth-order derivatives with respect to a set of normal coordinates $\{\hat{Q}_i\}$, at the equilibrium geometry, respectively. To further reduce the computational cost for multi-dimensional cases, an n-

mode coupling representation of QFF (nMR-QFF) was applied [23], which includes mode couplings up to n modes.

By taking each normal mode as the degree of freedom in the dynamics simulation, the Hamiltonian for QCD2 with nMR-QFF as the potential energy is

$$\hat{H}\left(\left\{\hat{P}_i\right\},\left\{\hat{Q}_i\right\}\right)=\sum_i \frac{\hat{P}_i^2}{2}+V_{\mathrm{QFF}}^{n-\mathrm{mode}}\left(\left\{\hat{Q}_i\right\}\right), \tag{45}$$

where $V_{QFF}^{n-\mathrm{mode}}$ denotes nMR-QFF. In this Hamiltonian we neglected the Watson term, which represents the vibrational-rotational coupling. Mass does not appear in the equations since the QFF normal coordinate is mass weighted. Therefore, the time evolution of variables of QCD2 with 1MR-QFF (general expressions are not shown for simplicity) is derived as

$$
\begin{aligned}
\dot{Q}_i &= P_i \\
\dot{P}_i &= -h_{ii}Q_i+\frac{t_{iii}}{2}\left(Q_i^2+\lambda_{2i,0i}\right)+\frac{u_{iiii}}{6}Q_i\left(Q_i^2+2\lambda_{2i,0i}\right) \\
\dot{\lambda}_{2i,0i} &= 2\lambda_{1i,1i} \\
\dot{\lambda}_{1i,1i} &= \lambda_{0i,2i}-\lambda_{2i,0i}\left[h_{ii}+t_{iii}Q_i+\frac{u_{iiii}}{2}\left(Q_i^2+\lambda_{2i,0i}\right)\right] \\
\dot{\lambda}_{0i,2i} &= -2\lambda_{1i,1i}\left[h_{ii}+t_{iii}Q_i+\frac{u_{iiii}}{2}\left(Q_i^2+\lambda_{2i,0i}\right)\right].
\end{aligned}
\tag{46}
$$

For molecules with more than 1 degree of freedom, we applied 3MR-QFF, because it has been shown by various examples that the 3MR-QFF is sufficient to describe fundamental modes as well as more complex overtone modes. The QCD2 and classical simulations were performed numerically with a fourth-order Runge-Kutta integrator. For formaldehyde (CH_2O) and formic acid (HCOOH), 3MR-QFF PES was generated at the level of MP2/aug-cc-pVTZ [24, 25] using GAMESS [26] and Gaussian03 [27] program packages. In this work, the results obtained by our method are compared with those by vibrational self-consistent field method (VSCF) with full second-order perturbation correction (VPT2), which is based on the quantum mechanics and accurate enough to treat molecular vibrations.

We here present results of the spectral analysis of trajectories obtained from the simulation that can be compared with other theoretical calculations and experimental results. The Fourier transform of any dynamical variables obtained from the trajectories of MD simulations is related to spectral densities. In particular, Fourier transform of velocity autocorrelation function gives the density of vibrational states. In addition, the power spectrum of the time series or autocorrelation function of each normal coordinate shows the contribution to frequency peaks of the spectrum obtained from velocity autocorrelation. Here we adopted the latter procedure. The time interval used was 0.1 fs and total time is 1 ps for all MD and

QCD simulations. The resolution in the frequency domain is less than 1 cm^{-1}, which is enough accuracy for the analysis of the molecular vibrations of interest. If a longer time trajectory is obtained, the resolution of the Fourier spectrum becomes fine.

Since each normal mode is taken as the degree of freedom explicitly in the present dynamics simulation, the interpretation and analysis of the results can directly be related with each normal mode. The results are shown in Table 1. The table indicates that the harmonic and QFF approximation of the PES results in a large deviation between each other. Therefore, anharmonicity of the potential must be considered to perform reliable simulations. The table shows that for the analysis of fundamental frequencies, the QCD2 has higher accuracy than the classical results, which can be compared with the VPT2 results in all cases. In spite of the high accuracy, the computational cost of the QCD2 remains low even when applied to larger systems. For HCOOH molecule, the QFF is so anharmonic that the classical simulation does not give clear vibrational frequencies due to the chaotic behavior of the power spectrum. The QCD may suppress the chaotic motion as seen in the full quantum mechanics.

	Mode	NMA	MD	QCD	VPT2	Exp.
H$_2$CO	ν_1	3040	2901	2843	2866	2843
	ν_2	2997	2868	2838	2849	2782
	ν_3	1766	1764	1723	1734	1746
	ν_4	1548	1504	1509	1515	1500
	ν_5	1268	1247	1250	1251	1250
	ν_6	1202	1166	N/A	1189	1167
HCOOH	ν_1	3739	N/A	3527	3554	3570
	ν_2	3126	N/A	2980	2989	2943
	ν_3	1794	N/A	1761	1761	1770
	ν_4	1409	N/A	1377	1385	1387
	ν_5	1302	N/A	1270	1231	1229
	ν_6	1130	N/A	1120	1097	1105
	ν_7	626	N/A	631	620	625
	ν_8 /ν_9	1058 /676	N/A	N/A	1036 /642	1033 /638

Table 1.

3.2. Proton transfer reaction in guanine-cytosine base pair

DNA base pairs have two and three inter-base hydrogen bonds for Adenine-Thymine and Guanine-Cytosine pairs, respectively. Proton transfer reactions among based were theoretically investigated by quantum chemical methods and further quantum mechanical analyses for decases [28-33]. In order to investigate dynamical stability of proton-transferred structures of the model system consisting DNA bases, we here perform QCD2 simulations of a model Guanine-Cytosine base pair. The model potential is given by

$$V^{\mathrm{GC}}\left(x,y,z\right) = \sum_{i,j,k} h'_{i,j,k} x^i y^j z^k, \tag{47}$$

where parameters in the model potential are given by Villani's paper [30, 31], which is fifth-order polynomials with respect to the coordinates for GC pairs and determined by the first principle calculations (B3LYP/cc-pVDZ). The reaction coordinates x, y, and z are shown in the figure. The corresponding quantal potentials are explicitly given by

$$\tilde{V}_2^{\mathrm{GC}}\left(x,y,z,\xi,\eta,\zeta\right) = \sum_{l,m,n=0}^{2} \sum_{i=0}^{5-2l} \sum_{j=0}^{5-2m} \sum_{k=0}^{5-2n} H_{i,j,k}^{l,m,n} x^i y^j z^k \left(\frac{\xi}{2}\right)^l \left(\frac{\eta}{2}\right)^m \left(\frac{\zeta}{2}\right)^n, \tag{48}$$

with

$$H_{i,j,k}^{l,m,n} = \frac{(i+2l)!}{i!l!} \frac{(j+2m)!}{j!m!} \frac{(k+2n)!}{k!n!} h'_{i+2l,j+2m,k+2n}, \tag{49}$$

where Greek characters denote the cumulant variables. In order to avoid the particles escaping from the bottoms, we have added the well-like potential is defined as

$$V_{\mathrm{well}}\left(\{q_i\}\right) = V_0 \left[1 + \prod_{i=x,y,z} \left(\theta_b\left(q_i - q_{i\max}\right) - \theta_b\left(q_i - q_{i\min}\right)\right)\right], \tag{50}$$

where $q_{i\max}$ and $q_{i\min}$ are maximum and minimum range of potential and V_0 is height of the well-like potential. An approximate Heaviside function is given by

$$\theta_b\left(x\right) = \frac{\mathrm{erf}\left(\sqrt{b}x\right)+1}{2}, \tag{51}$$

where b is an effective width of the approximate Heaviside function and guarantees smoothness of the potential. Using this approximate Heaviside function, the quantal potential for

the well-like potential is analytically derived. When V_0 is appropriately large, the particles stay around minima during dynamics simulations. We set $b = 100$, $q_{i\max} = 2.0(\text{Å})$, $q_{i\min} = 0.4(\text{Å})$, and $V_0 = 0.05$ (a.u.). Both $q_{i\max}$ and $q_{i\min}$ are in a reasonable range for the coordinate of the proton, because the distances between heavy elements (O and N) of the DNA bases are approximately 2.7~3.0 (Å) and roughly speaking the bond length of OH and NH are almost 1.0 ~ 1.1 (Å). The ordinary PES analysis gives both global and metastable structures for the GC pair. The former structure is the original Watson-Crick type and the latter is double proton-transferred one as easily found in (a) and (c). No other proton-transferred structure is found on the PES.

In the actual calculations, the time interval used was 0.1fs, total time is 2ps. The initial conditions of the variables can be determined by the least quantal energy principle. In figures 2 we have depicted phase space (x/px, y/py, z/pz) structures of a trajectory obtained by the QCD simulations. For cases (a) and (b), the dynamical feature of the closed orbits is the same except for its amplitudes. The phase space of the x/px is compact, on the other hand, that of z/pz is loose in comparison with that of y/py. The explicit isotope effects on the phase space structure are found in the cases of (c) and (d). In Fig. 2-(c), the nuclei initially located at the metastable structure go out from the basin and strongly vibrate around the global minimum due to tunneling. On the other hand, the deuterated isotopomer remains around the meta-stable structure. It is concluded that the metastable structure of the protonated isotopomer is quantum mechanically unstable, though it is classically stable based on the PES analysis. Therefore, it is important to take the quantum effects into isotope effects on the metastable structure with a small energy gap.
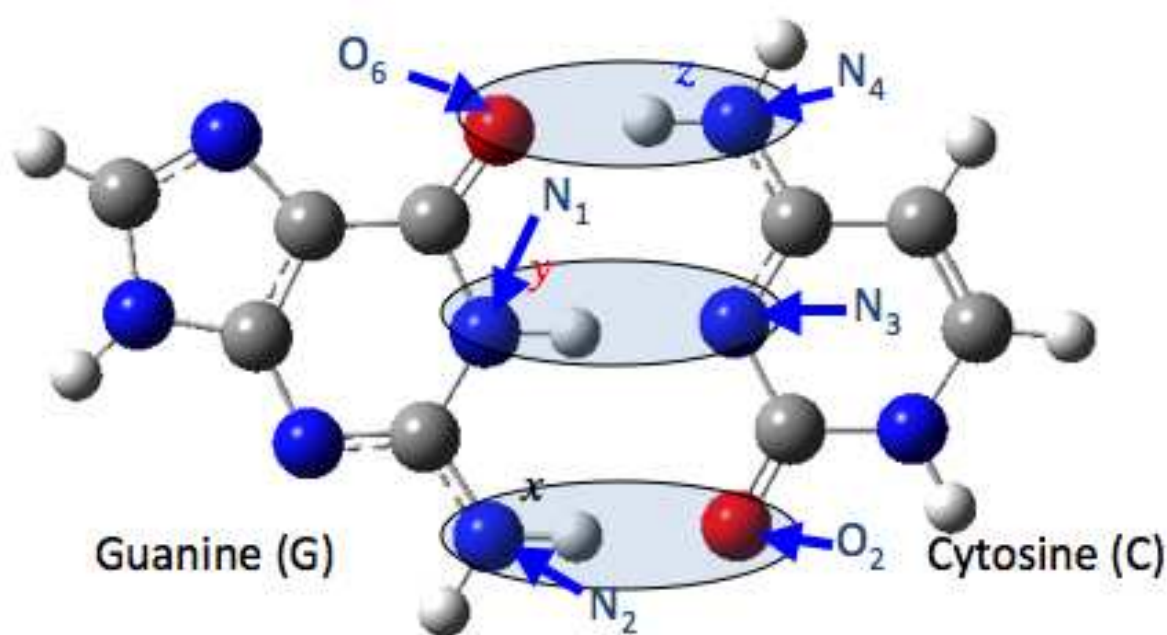

Figure 1. A Model for multiple proton transfer reactions in GC pairs. x, y, and z are reaction coordinates of the proton transfer reactions
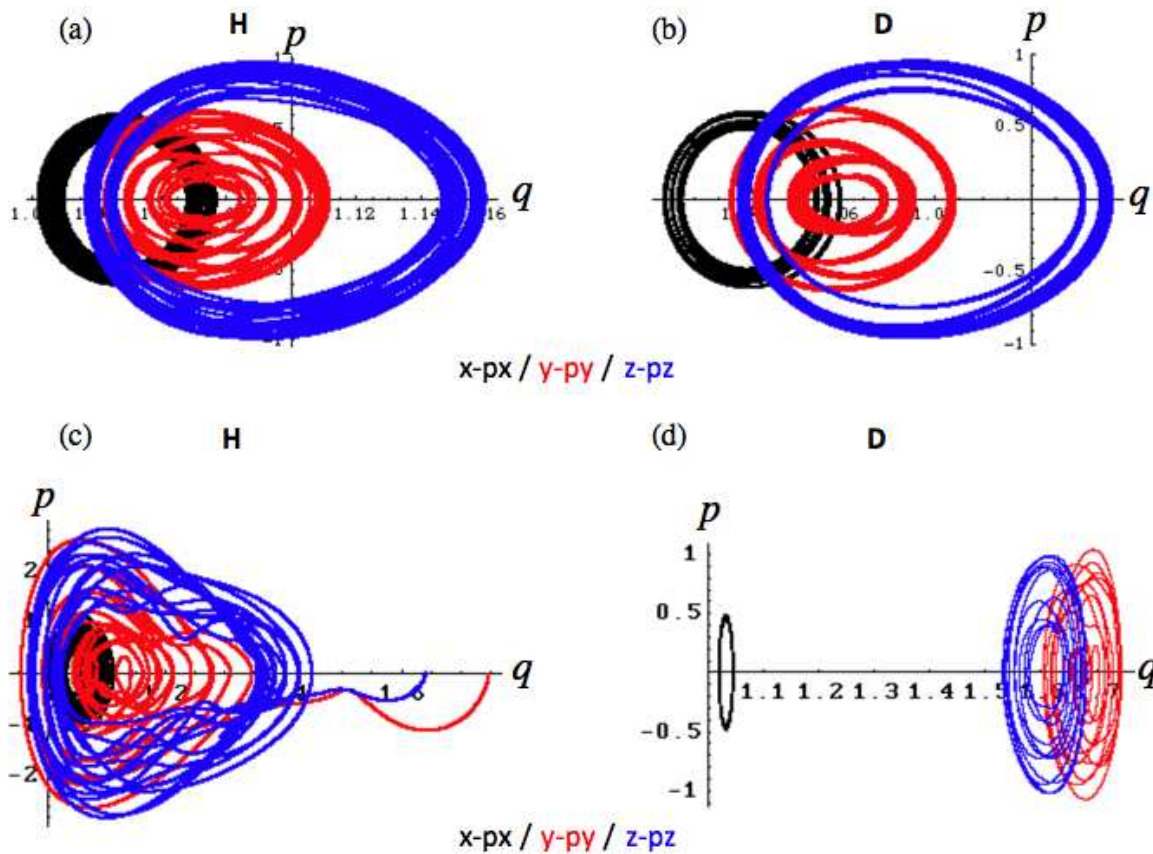
Figure 2. QCD phase space structures of the GC pair, where $q=x$, y, or z and $p=p_x$, p_y, or p_z, respectively. (a) and (b) are initially located around the global minimum for the protonated and deuterated cases. (c) and (d) are initially located around the metastable structure for the protonated and deuterated cases.

3.3. Quantal structural transition of finite clusters

Melting behavior of the finite quantum clusters were extensively investigated by many re-searchers using different kind of methodologies [34-39]. We here investigate the melting be-havior of n particle Morse clusters (abbreviated as M_n) by means of the QCD2 method. The Morse potential has following form:

$$V_M(r) = D_e\left[\exp\left(-2\rho\left(r - R_e\right)\right) - 2\exp\left(-\rho\left(r - R_e\right)\right)\right],\tag{52}$$

where D_e, R_e and ρ are parameters for a depth, a position of minimum, and a curvature of potential. In order to evaluate the quantal potential for the Morse potential, we adopt a Gaussian fit for the potential as

$$V_G(r) = \sum_{i=1}^{N_G} c_i e^{-\alpha_i r^2},\tag{53}$$

which has an analytic form of the quantal potential and coefficients $\{c_i\}$ are obtained by a least square fit for a set of even-tempered exponent with upper and lower bounds ($\alpha_{upper}=10^6$ and $\alpha_{lower}=10^{-3}$). By choosing the number of Gaussians, N_G, the set of the coefficients is explicitly determined and we here set $N_G=41$.

We here evaluate optimized structures of M_n clusters (n=3-7) for $D_e=1$, $R_e=1$, and $\alpha=1$. The classical global minimum structures of M_3, M_4, M_5, M_6, and M_7 structure have C_{3v}, T_d, D_{3h}, O_h, and D_{5h} symmetry respectively. Table 2 lists energy for each method. We found that the diagonal approximation causes the artificial symmetry breaking and the spherical approximation gives less accurate results. Original approximation gives the most accurate and correctly symmetric global minimum structures. The diagonal approximation gives the same results by the original one for M_6 due to the same reason denoted before. The error of both the diagonal and spherical approximation decreases with the increase of the number of the particles. It is expected that both approximations work well for many particle systems instead of the original one. In particular the error of the diagonal approximation is 0.006 % for the M_7 cluster. This fact tells us that the diagonal approximation is reliable for the M_7 cluster at least the stable structure.

For the analyses on quantum melting behavior, the parameters of the Morse potential are chosen as $D_e=1$, $R_e=3$, and $\alpha=1$. Table 2 also lists nearest and next nearest distances obtained by the original and classical ones. As found in this Table, all the distances elongate with respect to classical ones. For example, the distances of M_3 and M_4 elongate by 7.2% and 7.8%, respectively. It is notable that these distances does not equally elongate. The ratio between the original and classical ones is different for the nearest and next nearest distances, i.e. 8.16% and 6.20% for M_5, 7.36% and 3.91% for M_6, and 8.70% and 6.79% for M_7, respectively. In future works, we investigate influence of these behaviors on the structural transition (deformation) of the quantum Morse clusters in detail.

In order to measure the melting behavior of the finite clusters, we here use the Lindemann index defined as

$$\sigma = \frac{2}{N(N-1)}\sum_{ij}\frac{\sqrt{\langle r_{ij}^2\rangle - \langle r_{ij}\rangle^2}}{\langle r_{ij}\rangle}, \tag{54}$$

where $\langle r_{ij}\rangle$ is a long time-averaged distance between i and j-th particles. In the present approach, there exist two possible choices of the average. One is the quantum mechanical average within the second-order QCD approach, $\langle r_{ij}\rangle_{QCD2}=\langle|\hat{q}_i-\hat{q}_j|\rangle_{QCD2}$, which include information of both the classical position and the second-order position cumulant simultaneously, and the other is the average evaluated by means of the classical positions appearing in the QCD approach, $\langle r_{ij}\rangle=\langle|q_i-q_j|\rangle$. We perform real-time dynamics simulation to obtain the Lindemann index for both systems, where we adopt $m=100$.

The Lindemann indexes obtained by CD and QCD are illustrated in Fig. 1. In the figure, there exist three different regions. Until a freezing point, the Lindemann index gradually increases as the increase of the additional kinetic energy. In this region, the structural transition does not actually occur and the cluster remains stiff. This phase is called "solid-like phase". On the other hand, above a melting point, the structural transition often occurs and the cluster is soft. This phase is called "liquid-like phase". Between two phases, the Lindemann index rapidly increases. This phase is referred as "coexistence phase", which is not allowed for the bulk systems and peculiar to the finite systems. For both the solid- and liquid-like phases, the Lindeman index does not deviate too much. However that of the coexistence phase fluctuates due to a choice of the initial condition. In comparison with CD and QCD results, the transition temperatures of QCD are lower than those of the CD reflecting the quantum effects. The freezing and melting temperatures are about 0.35 and 0.42 for QCD and about 0.41 and 0.60 for CD, respectively. Since the zero-point vibrational energy is included in QCD, the energy barrier between the basin and transition state become lower so that the less temperature is needed to overcome the barrier. This is so-called quantum softening as indicated by Doll and coworker for the Neon case by means of the path-integral approach. Our real-time dynamics well reproduce their tendency for this static property. On the other hand, behavior of Lidemann indexes from $\langle \hat{r}_{ij} \rangle_{QCD2} = \langle | \hat{q}_i - \hat{q}_j | \rangle_{QCD2}$ and $\langle r_{ij} \rangle = \langle | q_i - q_j | \rangle$ is slight different, whereas the transition temperature is the same. In the solid-like phase the Lindemann index obtained by the classical dynamics is equivalent to that of the classical contribution from QCD approach. On the other hand, in the liquid-like phase the Lindemann index is equivalent to that by the classical dynamics. This fact originates from the fact that the high temperature limit of the quantum results coincides with that of the classical one. It is stressed here that the cumulant variables, which contributes to not only to the quantum delocalization but also to the thermal fluctuation.

	Energy				Distance	
	Spherical	Diagonal	Original	Classical	Original	Classical
M$_3$	-2.52135	-2.55978	-2.56510	-3.00000	1.07198	1
M$_4$	-5.20344	-5.22683	-5.24237	-6.0000	1.07811	1
M$_5$	-8.71392	-8.74464	-8.76049	-9.85233	0.99212 1.15085	0.91725 1.08364
M$_6$	-13.1836	-13.2141	-13.2141	-14.7182	1.00473 1.37518	0.93581 1.32343
M$_7$	-18.4016	-18.4404	-18.4415	-20.3282	0.88288 1.01263	0.81221 0.948237

Table 2. Nearest and next nearest distances and energy for global minimum obtained by cumulant and classical dynamics for 3-dimensional M$_n$ clusters (n=3-7).
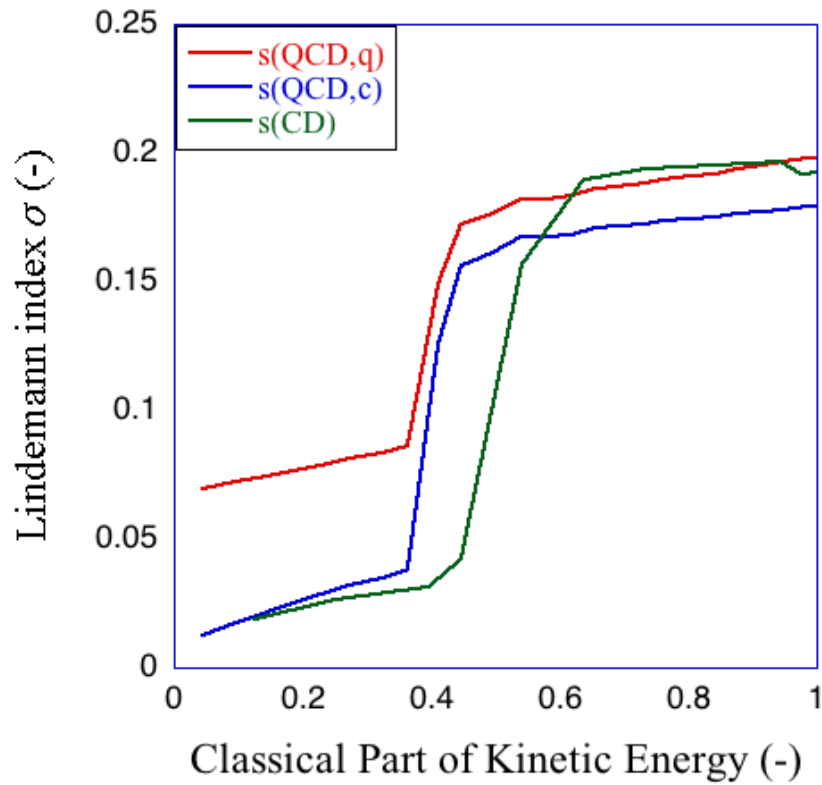
Figure 3. Static Lindemann indexes evaluated from QCD quantum distance (red), QCD classical distance (blue), and CD classical distance (green).

4. Summary

As an extension to the mechanics concerning about Ehrenfest theorem, we formulated a quantal cumulant mechanics (QCM) and corresponding dynamic method (QCD). The key point is the use of a position shift operator acting on the potential operator and introducing the cumulant variables to evaluate it, so that one need not truncate the potential, and it does not require separating into quantum and classical parts. In particular, we derived the coupled equation of motion (EOM) for the position, momentum, and second-order cumulants of the product of the momentum and position fluctuation operators. The EOM consists of variables and a quantal potential and its derivatives, where the quantal potential is expressed as an exponential function of the differential operator acting on the given potential. We defined density and joint density evaluated from the cumulant expansion scheme. It is clearly found that the present second-order approach gives a Gaussian density distribution spanned both on position and momentum space. Since the density is normalized, the joint density is considered exactly as probability distribution. We also indicated the relation between the joint density and cumulant variables as expectation values calculated from the distribution. We extended the QCD for the one-dimensional system in to treat the multi-dimensional systems. We derived the EOMs with the 24N dimensional phase space.

As numerical examples, we performed four applications to the simple systems. The first is the application to molecular vibrations. At first we showed that the normal mode analysis is extended to the effective potential appeared in the QCD. We illustrated that the anharmonic contribution is taken into account through mixing between the ordinary and the extended coordinates. The QCD simulations for the *ab initio* derived quartic force field are performed. The vibrational frequencies obtained from its power spectrum are good agreement with those obtained by accurate methods such as VPT2 and VCI.

The second is the proton transfer reactions in model DNA base pairs. We numerically showed the geometric isotope effects on the stability of the proton-transferred structures of the DNA base pairs as a function of the mass. We performed QCD simulations in order to investigate dynamical stability of the proton-transferred GC pair. The results showed that the proton-transferred structure of the protonated isotopomer is dynamically unstable and that of deuterated isotopomer remains stable. In former case, dynamically induced transition from the metastable to global minimum occurs. It is relevant to include dynamical effects to treat quantum isotope effects on the proton transfer reactions.

The last application is structural transition of finite quantum Morse clusters. We first compared the energy of the stable structures of the classical M_n cluster with those of quantum counterpart and found that the quantum effects due to zero point vibration is remarkable for small system and suppressed for larger. Then we performed the real-time dynamics to evaluate the Lindemann index to characterize the dynamical effects on the melting for M_7 cluster. In between solid-like and liquid-like phases (so-called coexistence phase), structural changes of the cluster occur intermittently.

Acknowledgements

Author details

Yasuteru Shigeta[1,2]

1 Department of Materials Engineering Science, Graduate School of Engineering Sciences, Osaka University, Machikaneyama-cho, Toyonaka, Osaka, Japan

2 Japan Science and Technology Agency, Kawaguchi Center Building, Honcho, Kawaguchi-shi, Saitama, Japan

References

[1] Schrödinger, E. (1926). Quantisierung als Eigenwertproblem (Erste Mitteilung). Annalen der Physik, Vol. 79, No. 4, (April, 1926), pp. 361-376. ISSN: 0003-3804

[2] Schrödinger, E. (1926). Quantisierung als Eigenwertproblem (Zweite Mitteilung). Annalen der Physik, Vol. 79, No. 6, (May, 1926), pp. 489-527. ISSN: 0003-3804

[3] Schrödinger, E. (1926). Quantisierung als Eigenwertproblem (Dritte Mitteilung: Storungstheorie, mit Anwendung auf den Starkeffekt der Balmerlinien). Annalen der Physik, Vol. 80, No. 13, (September, 1926), pp. 437-490. ISSN: 0003-3804.

[4] Schrödinger, E. (1927). Quantisierung als Eigenwertproblem (Vierte Mitteilung). Annalen der Physik, Vol 81, No. 18, (September, 1927), pp. 109-139. 0003-3804.

[5] Heisenberg, W. (1943). The observable quantities in the theory of elementary particles. III. Zeitschrift für physik, Vol 123, No. 1-2, (March, 1943) pp. 93-112. ISSN: 0044-3328.

[6] Ehrenfest, P. (1927). Bemerkung über die angenäherte Gültigkeit der klassischen Mechanik innerhalb der Quantenmechanik. Zeitschrift für physik, Vol 45, No. 7-8, (July, 1927), pp. 455-472. ISSN: 0044-3328.

[7] Prezhdo, O.V. & Pereverzev, Y.V. (2000). Quantized Hamilton dynamics. Journal of Chemical Physics, Vol. 113, No. 16, (October 22, 2000), pp. 6557-6565. ISSN: 0021-9606.

[8] Prezhdo, O.V. (2006). Quantized Hamilton Dynamics. Theoretical Chemistry Accounts, Vol. 116, No. 1-3, (August 2006), pp. 206-218. ISSN: 1432-881X and references cited therein.

[9] Miyachi, H.; Shigeta, Y.; Hirao K. (2006). Real time mixed quantum-classical dynamics with ab initio quartic force field: Application to molecular vibrational frequency analysis. Chemical Physics Letters, Vol. 432, No. 4-6, (December 11, 2006) 585-590. ISSN: 0009-2614

[10] Shigeta, Y.; Miyachi, H.; Hirao, K. (2006). Quantal cumulant dynamics: General theory. Journal of Chemical Physics, Vol. 125: 244102. ISSN: 0021-9606.

[11] Shigeta, Y.; Miyachi, H.; Hirao, K. (2007). Quantal cumulant dynamics II: An efficient time-reversible integrator. Chemical Physics Letters, Vol. 443, No. (AUG 6 2007), 414-419. ISSN: 0009-2614

[12] Shigeta Y. (2007). Quantal Cumulant Dynamics for Dissipative Systems. AIP proceedings Vol. 963, (2007), 1317.

[13] Shigeta Y. (2008). Quantal cumulant dynamics III: A quantum confinement under a magnetic field. Chemical Physics Letters, Vol. 461, No. 4-6, (August 20, 2008), 310-315. ISSN: 0009-2614

[14] Shigeta Y. (2008). Distribution function in quantal cumulant dynamics. Journal of Chemical Physics, Vol. 128, No. 16, (April 28, 2008) 161103. ISSN: 0021-9606.

[15] Shigeta, Y.; Miyachi, H.; Matsui, T.; Hirao, K. (2008) Dynamical quantum isotope effects on multiple proton transfer reactions. Bulletin of the Chemical Society Japan. Vo. 81, No. 10, (October 15, 2008), 1230 -1240. ISSN: 0009-2673.

[16] Pereverzev, Y.V.; Pereverzev, A.; Shigeta, Y.; Prezhdo, O.V. (2008) Correlation functions in quantized Hamilton dynamics and quantal cumulant dynamics. Journal of Chemical Physics, Vol. 129, No. 14, (October 14, 2008), 144104. ISSN: 0021-9606.

[17] Shigeta, Y. Molecular Theory Including Quantum Effects and Thermal Fluctuations, the Bulletin of Chemical Society Japan, Vo. 82, No. 11, (November 15, 2009), 1323-1340. ISSN: 0009-2673.

[18] Shigeta, Y.; Miyachi, H.; Matsui, T.; Yokoyama, N.; Hirao, K. "Quantum Theory in Terms of Cumulant Variables", Progress in Theoretical Chemistry and Physics, Vol. 20, "Advances in the Theory of Atomic and Molecular Systems - Dynamics, Spectroscopy, Clusters, and Nanostructures", edited by Piecuch, P.; Maruani, J.; Delgado-Barrio, G.; Wilson, S., pp. 3-34, Springer, 2009, 3-34.

[19] Shigeta, Y.; Inui, T.; Baba, T.; Okuno, K.; Kuwabara, H.; Kishi, R.; Nakano, M. (2012) International Journal of Quantum Chemistry. in press, (2012). ISSN: 0020-7608.

[20] Mayer, J. E. (1937). The Statistical Mechanics of Condensing Systems I. Journal of Chemical Physics, Vol. 5, (January, 1937), 67-73. ISSN: 0021-9606.

[21] Kubo, R. (1962). Generalized Cumulant Expansion Method. Journal of Physical Society of Japan, Vol. 17, No. 7, (July, 1962) 1100-1120. ISSN: 0031-9015.

[22] Mandal. S.H.; Sanyal, G.; Mukherjee, D. (1998). A Thermal Cluster-Cumulant Theory. Lecture Notes in Physics, Vol. 510, (1998), 93-117. ISSN: 0075-8450.

[23] Yagi, K.; Hirao, K.; Taketsugu, T.; Schmidt, M.W.; Gordon, M.S. (2004). *Ab initio* vibrational state calculations with a quartic force field: Applications to H_2CO, C_2H_4, CH_3OH, CH_3CCH, and C_6H_6. *Journal of Chemical Physics*, Vol. 121, No. 3 (July 15, 2004) 1383-1389. ISSN: 0021-9606.

[24] Möller, C; Plesset, M.S. (1934). Note on an approximation treatment for many-electron systems. *Physical Review,* Vol. 46, No. 7, (October, 1934), 618-622. ISSN: 0031-899X.

[25] Lendall, R.A.; Dunning Jr, T.H.; Harrison, R.J. (1992). Electron affinities of the first-row atoms revisited. Systematic basis sets and wave functions. *Journal of Chemical Physics*, Vol. 96, No. 9, (May 1, 1992), 6796-6806. ISSN: 0021-9606.

[26] M.W. Schmidt et al (1993) General Atomic and Molecular Electronic-structure System. *Journal Computational Chemistry*, Vol. 14, No. 11, (November, 1993), 1347-1363. ISSN: 0192-8651.

[27] M.J. Frisch et al (2004) Gaussian 03 (Revision C.02). Gaussian Inc Wallingford CT

[28] Florián, J.; Hrouda, V.; Hobza, P. (1994). Proton Transfer in the Adenine-Thymine Base Pair. *Journal of the American Chemical Society*, Vol. 116, No. 4, (February 23, 1994), 1457-1460. ISSN: 0002-7863.

[29] Floriaán J, Leszczyn'sky J (1996) Spontaneous DNA Mutation Induced by Proton Transfer in the Guanine-Cytosine Base Pair: An Energetic Perspective. *Journal of the American Chemical Society*, Vol. 118, No. 12, (March 27, 1996), 3010-3017. ISSN: 0002-7863.

[30] Villani G (2005) Theoretical investigation of hydrogen transfer mechanism in adenine-thymine base pair. *Chemical Physics*, Vol. 316 No. 1-3, (September 19, 2005), 1-8. ISSN: 0301-0104.

[31] Villani G (2006) Theoretical investigation of hydrogen transfer mechanism in the guanine-cytosine base pair *Chemical Physics*, Vol. 324, No. 2-3, (MAY 31 2006), 438 -446. ISSN: 0301-0104.

[32] Matsui T, Shigeta Y, Hirao K (2006) Influence of Pt complex binding on the guanine cytosine pair: A theoretical study. *Chemical Physics Letters*, Vol. 423, No 4-6, (June 1, 2006), 331-334. ISSN: 0009-2614.

[33] Matsui, T.; Shigeta, Y.; Hirao, K. (2007). Multiple proton-transfer reactions in DNA base pairs by coordination of Pt complex. *Journal of Chemical Physics B*, Vol. 111, No. 5, (February 8, 2007), 1176-1181. ISSN: 1520-6106.

[34] Ceperley, D.M. (1995). Path-integrals in the theory of condensed Helium. *Review Modern Physics*, Vol. 67, No. 2, (April 1995), 279-355. ISSN: 0034-6861.

[35] Chakravarty, C. (1995). Structure of quantum binary clusters. *Physical Review Letters*, Vol. 75, No. 9, (August 28, 1995), 1727-1730. ISSN: 0031-9007.

[36] Chakravarty, C. (1996). Cluster analogs of binary isotopic mixtures: Path integral Monte Carlo simulations. *Journal of Chemical Physics*, Vol. 104, No. 18, (May 8, 1996), 7223-7232. ISSN: 0021-9606.

[37] Predescu, C.; Frantsuzov, P.A.; Mandelshtam, V.A. (2005). *Journal of Chemical Physics*, Vol. 122, No. 15, (April 15, 2005), 154305. ISSN: 0021-9606.

[38] Frantsuzov, P.A.; Meluzzi, D.; Mandelshtam, V.A. (2006). Structural transformations and melting in neon clusters: Quantum versus classical mechanics. *Physical Review Letters*, Vol. 96, No. 11, (March 24, 2006), 113401. ISSN: 0031-9007

[39] Heller, E. J. (1975). Time-dependent approach to semiclassical dynamics. *Journal of Chemical Physics*, Vol. 62, No. 4, (1975), 1544-1555. ISSN: 0021-9606.